AIAA 99-0754

Numerical Study of Wake Vortex Interaction with the Ground Using the Terminal Area Simulation System

Fred H. Proctor
NASA Langley Research Center
Hampton, VA

Jongil Han
North Carolina State University
Raleigh, NC

37th Aerospace Sciences Meeting & Exhibit
January 11-14, 1999 / Reno, NV

AIAA-99-0754

Numerical Study of Wake Vortex Interaction with the Ground Using the Terminal Area Simulation System

Fred H. Proctor*
NASA Langley Research Center
Hampton, Virginia

Jongil Han†
North Carolina State University
Raleigh, NC

Abstract

A sensitivity study for the "in-ground effect" on aircraft wake vortices has been conducted using a validated large eddy simulation model. The numerical results are compared with observed data and show good agreement for vortex decay and lateral vortex transport. The vortex decay rate is strongly influenced by the ground, but appears somewhat insensitive to ambient turbulence. In addition, the results show that the ground can affect the trajectory and descent-rate of a wake-vortex pair at elevations up to about 3 b_o (where b_o is the initial vortex separation). However, the ground does not influence the average circulation of the vortices until the cores descend to within about 0.6 b_o, after which time the ground greatly enhances their rate of demise. Vortex rebound occurs in the simulations, but is more subtle than shown in previous numerical studies.

Also described in this paper is the model formulation for surface stress, which is based on Monin-Obukhov similarity theory.

*Research Scientist, Flight Management and Control Division, AIAA member

†Research Scientist, Department of Marine, Earth, and Atmospheric Sciences

Nomenclature

B	aircraft wing span
b_o	initial vortex separation - $\pi B/4$
g	acceleration due to gravity
Z_i	initial height above ground of wake vortex
M	mass of generating aircraft
t	time coordinate
T^*	nondimensional time - $t\, V_o / b_o$
V_a	airspeed of generating aircraft
V_o	initial vortex descent velocity - $\Gamma_o/(2\,\pi\, b_o)$
z	vertical coordinate
z_o	ground roughness coefficient
Γ	vortex circulation
Γ_o	initial circulation - $M\,g/(b_o\,\rho\,V_a)$
ρ	air density
ϵ	turbulence (eddy) dissipation rate
ν	kinematic viscosity
η	nondimensional eddy dissipation - $(\epsilon\, b_o)^{1/3}\, V_o^{-1}$

I. Introduction

The behavior of aircraft wake vortices is being investigated by NASA in order to develop a predictor system that will safely reduce aircraft spacing and increase airport capacity.[1,2] This system, the Aircraft VOrtex Spacing System (AVOSS), includes prediction algorithms[3] for wake vortex transport and decay. In order to protect the AVOSS approach/departure corridor, these algorithms must function in real time and at altitudes where the ground can affect vortex behavior. In order to develop this system, the influence of both the weather and the ground surface needs to be understood and quantified. Investigations with a Large Eddy Simulation (LES) numerical model are in progress and are intended to support the development of the predictor system.[4]

Some understanding of wake vortex behavior near the ground has been achieved in past research efforts,[5,6,7,8,9,10,11,12] but much more information is needed in order to develop prediction algorithms that can be applied successfully near the ground. Previous research has shown that, when near the ground, the transport of wake vortices is affected by both viscous and inviscid processes.[13] As a vortex pair descends toward the ground, inviscid processes cause the vortices to lose their vertical motion and diverge laterally.[14] This effect can be modeled mathematically by placement of image vortices beneath the ground plane so as to satisfy impermeable and free-slip conditions at the ground. However, this effect alone cannot explain the vortex rebounding that is often observed near the ground. A second influence is caused by the viscous retardation of the flow next to the ground. As the vortex circulation comes in contact with the ground, friction creates a shear layer of opposite sign vorticity, which is then swept upward and around the infringing vortex. This shear layer wraps into secondary vortices, which then act on the primary vortex causing it to rise or rebound upwards.[5] Another effect from the frictional retardation of the flow next to the ground is to weaken the coupling with the sub-surface images, which in turn, reduces the rate at which the vortices spread, as otherwise predicted by inviscid theory. Further complications for the prediction of the wake vortex trajectory are due to the presence of ambient crosswind near the ground which can influences the position and intensity of the secondary vortices.[10,11]

Vortex decay near the ground is known to be enhanced by proximity to the ground, but details are not well understood.[15] Little is known about the influence of environmental turbulence on wake vortex behavior near the ground. For aircraft wake vortices away from the ground, ambient atmospheric turbulence has been recognized to be a key factor for the enhancement of the vortex decay.[16,17,18,19,20,21] At low altitudes, however, the interaction of the vortices with the ground may be a more important factor for vortex decay.

Based on the previous wake vortex research efforts, Corjon *et al*[22] and Robins *et al*[3] have modified Greene's model[23] (which is applicable to the free atmosphere) for ground effects. Robins *et al* define a wake vortex to be "in-ground-effect" (IGE) when viscous effects with the ground are significant. This should occur when the vortex core descends to within $z < b_o$. They also define wake vortices to be "out-of-ground effect" (OGE) -- when the vortices are far from the influence of the ground; and "near-ground effect" (NGE) -- when the vortices are close enough to have some influence from the ground, but far enough not to generate secondary vorticity. The region defined by NGE is above where ground-viscous effects are significant, but where inviscid process due to the ground can act to reduce the vortex sink rate ($b_o < z < 3\, b_o$). The influence of the ground at these various altitudes must be carefully studied in order to insure the development of valid predictive algorithms.

In the present study, a three-dimensional numerical LES is conducted for a landing L-1011 which was observed at 20:09 UTC on 26 September 1997 at Dallas-Fort Worth (DFW) airport.[24] This specific case was chosen at the recommendation of Northwest Research Associates, [25] who are analyzing the NASA deployment data and are developing an AVOSS wake-vortex prediction model. Also presented are additional sensitivity experiments conducted for a wide range of ambient turbulence intensities and for a range of wake generation heights. Simulation results, including comparisons with Lidar measurements, are presented in section 3. The numerical model and initial conditions are briefly described in section 2, and the conclusions of this study are summarized in section 4.

II. The Model and Initial Conditions

The numerical model used in the present study is a three-dimensional, compressible, nonhydrostatic LES model called the Terminal Area Simulation System[26] (TASS), which has been adapted for simulation of wake vortex interaction with the atmosphere.[27] Grid-scale turbulence is explicitly computed while the effects of subgrid-scale turbulence is explicitly modeled by a conventional 1st-order closure model with modifications for stratification and flow rotation. All simulations are conducted assuming rotational Reynolds numbers (Γ_o/ν) of ~10^7. The numerical formulation of the TASS model is computationally efficient and essentially free of numerical diffusion.[28]

One feature of TASS, which enhances its ability to correctly simulate wake vortex behavior near the ground, is its formulation for the ground boundary condition. The formulation is based on Monin-Obukhov similarity theory, with the subgrid stress at the ground determined locally from the wind speed, surface roughness, and the local thermal stratification. Details of the formulation are described in the appendix.

In recent studies with the TASS model Han *et al*[21,29] have examined wake vortex decay and the development of Crow instability within a Kolmogorov spectrum of homogeneous atmospheric turbulence. In these studies, periodic boundary conditions are imposed at all domain boundaries in order to avoid the effects of the ground. In the present study, we include the ground surface, with periodic boundary conditions only at the horizontal

boundaries. As before, preexisting resolved-scale ambient turbulence is generated prior to injecting a wake vortex pair.

Table 1. *Initial vortex parameters.*

Parameter	Value
Vortex spacing (b_o)	37 m
Generating height (Z_i)	14 m (0.38 b_o)
Vortex circulation (Γ_o)	390 m^2 s^{-1}
Vortex core radius	3 m (b_o/12.3)

The initial vortex system represents a post roll-up, wake-vortex velocity field as described in Proctor[4], and consists of a pair of counter-rotating vortices that have no initial variation in the axial direction. The initial vortex parameters (Table 1) are from the observed aircraft parameters for the L-1011. Note that the initial vortex elevation is less than half of initial vortex separation and is well within IGE.

Table 2. *Model domain parameters.*

Parameter	Value
Crossplane width	370 m (10 b_o)
Crossplane height	81 m (2.2 b_o)
Axial length	81 m (2.2 b_o)
Crossplane grid resolution	1.5 m (b_o / 24.7)
Axial grid resolution	2.0 m
Ground roughness (z_o)	0.1 m

The model domain parameters are given in Table 2. The relatively small domain size in the axial direction is assumed in order to save computing time and simplify analysis of the results. This truncated size will suppress the development of Crow instability, which has a theoretical maximum wavelength of about 8.6 b_o.[30] Thus, statistically homogeneous wake vortex decay behavior is anticipated along the axial direction. The domain width of 10 b_o in the crossflow direction is sufficiently large to minimize boundary influences. The domain size in the vertical direction (2.2 b_o) is large enough to investigate IGE, but bounds the largest resolvable turbulence eddy size, so that the effects of large turbulent eddies (such as thermals) on vortex transport are not taken into account.

Table 3. *Ambient turbulence energy dissipation rate and corresponding dimensionless turbulence intensity for the sensitivity cases (baseline case in bold).*

ϵ (m^2 s^{-3})	η
3.317 x 10^{-8}	0.0014
3.317 x 10^{-5}	0.0638
1.654 x 10^{-3}	**0.2349**
6.671 x 10^{-3}	0.3739

The ambient temperature and velocity profiles for the selected case study are given in Figure 1. The atmosphere for this case has near-neutral stratification, with the static stability being very slightly unstable near the ground. The crossflow velocity is somewhat weak over the vertical depth of the simulation, with an average value of about 1 *m/s*.

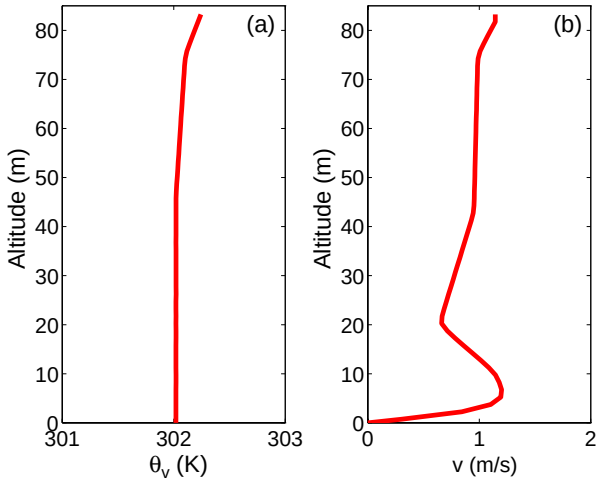

Figure 1. *Initial profile of a) ambient potential temperature and b) crosswind for DFW, 26 September 1997, 20:09 UTC.*

Prior to injecting the initial wake-vortex field, the initial turbulence field is allowed to develop under an artificial external forcing of horizontal velocity at low wavenumbers. The forcing is applied along each horizontal plane using a two-dimensional Fast Fourier Transform (see references [21, 29] for other details). At the same time, the horizontal domain average temperature and velocity fields are forced to maintain their initial vertical profiles by subtracting the difference every time step. This approach allows a well-developed turbulent flow field which possess Kolmogorov's inertial subranges, and maintains the ambient temperature and wind profile. Once the turbulence is well developed, the vortex system is injected into the simulation and the external forcing is discontinued. The above approach differs from the one used in a companion paper,[31] in which the resolved-scale ambient turbulence is grown by boundary layer forcing rather than by an artificial forcing function as in this paper.

In order to evaluate the sensitivity to environmental turbulence, ambient turbulence fields are generated for four levels of turbulence. Their associated values of turbulence energy (eddy) dissipation rate, ϵ, are estimated from the well-known technique of fitting the inertial subrange of the simulated spectra. Their values and

corresponding nondimensional turbulence strengths, η, are given in Table 3. For the initial vortex parameters of this case, the range of values for η span typical values found in the lower atmosphere which range from about 0.01 in the nighttime to about 0.3 in the daytime.[4] The ambient turbulence field with a value of, $\epsilon = 1.654 \times 10^{-3}$ $m^2 s^{-3}$ (η =0.2349), is close to the value observed at 40 *m* elevation near the time of the L-1011 event. Thus, this numerical simulation can be directly compared with the Lidar wake-vortex measurements. [This case will be referred to as the baseline case.] Three-dimensional wake vortex simulations are carried out with each of the four turbulence fields identified in Table 3, with all other conditions identical. In addition to these experiments, a two-dimensional simulation is conducted with no ambient turbulence. In this experiment, the wake vortex can only decay from *two-dimensional turbulence* induced by the interaction of the vortex with the ground and atmosphere.

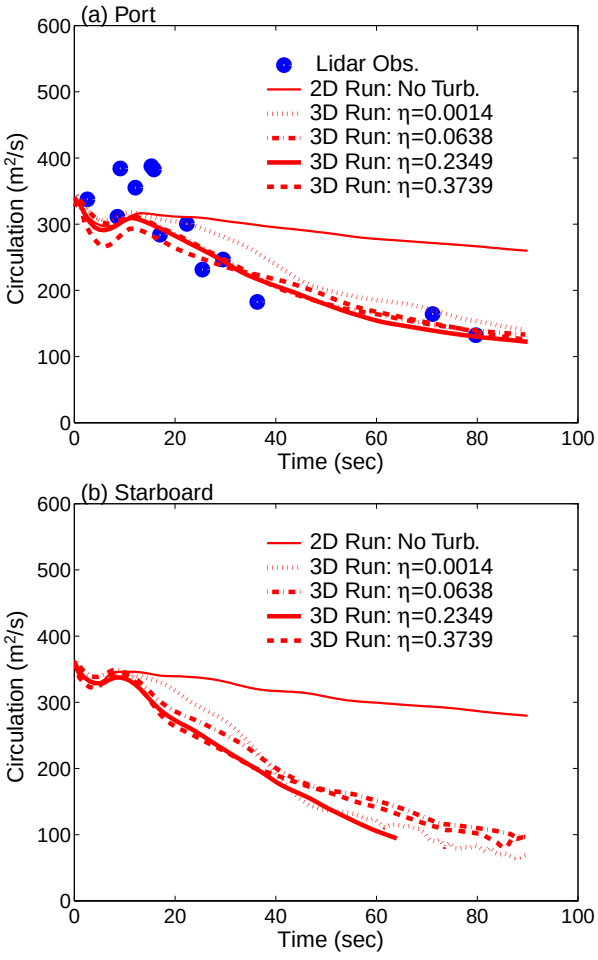

Figure 2. *Time evolution of 5-15 m averaged circulation for: a) port vortex and b) starboard vortex.*

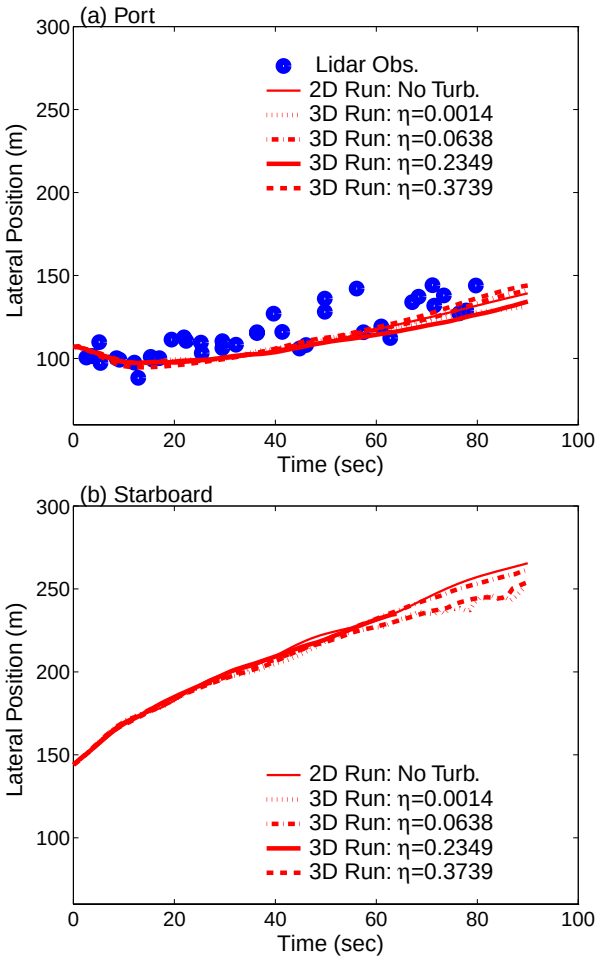

Figure 3. *Same as Fig. 2, but for lateral position.*

III. Numerical Results

Results from the five experiments with the conditions listed in Tables 1-3 are compared in Figures 2-4. The profiles for both starboard and port vortices are shown since the light crosswind (Fig.1) causes slight differences in their behavior. Lidar observations for the port vortices are shown for comparison (observations for the starboard vortex were unavailable). The four 3-D cases with various levels of ambient turbulence only show minor differences, and are in agreement with the Lidar data for lateral position and circulation decay. Note that the port vortex essentially stalls near the flight path and may be hazardous to other aircraft trailing close behind.

Specifically, Fig 2 shows a comparison of the average circulation (averaged over a radius between 5 and 15 *m* from the vortex center). A slight dip in average circulation occurs at early simulation times due to the vortex height being less than 15 *m* (the calculation of

circulation from the TASS data is clipped at the ground). The initially large values of average circulation from the Lidar observation are known overestimates that frequently occur during the first several seconds of measurements.[32] Note from Fig. 2 that the circulation decay is quite significant, even for the very-weak ambient turbulence case (η=0.0014). However, for the 2-D case with no ambient turbulence, very little decay occurs. Therefore, it appears that some small perturbations are necessary in order to promote vortex decay within IGE, even though the rate of decay is very weakly related to the ambient level of turbulence.

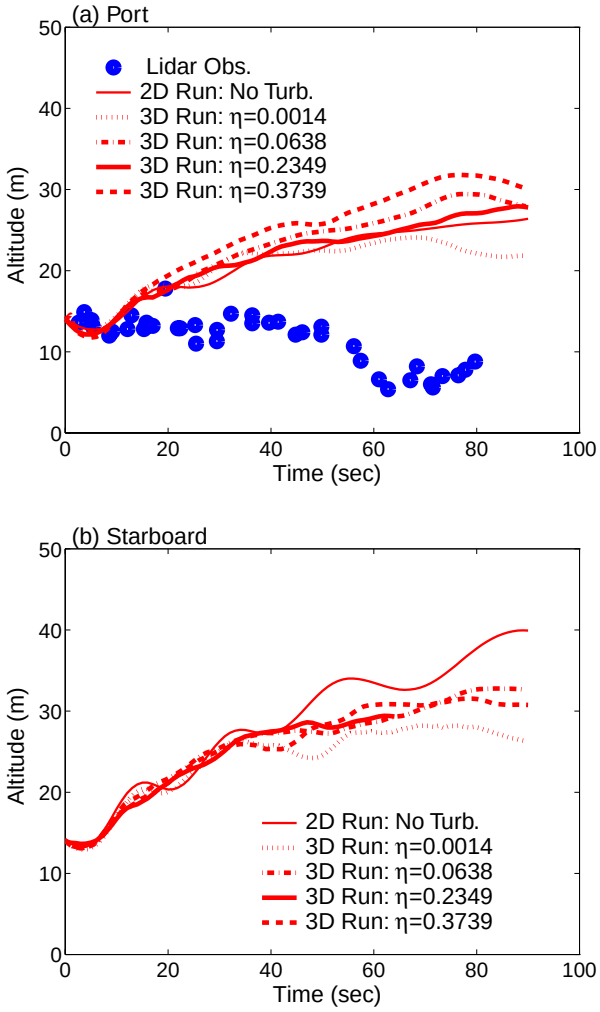

Figure 4. *Same as Fig. 2, but for vertical position.*

The lateral positions of the vortices are shown in Fig. 3. The Port (upstream) vortex initially travels upstream then slowly drifts downstream. However, its position remains within 30 *m* of the flight path during most of its lifetime. All of the simulations, including the 2-D no-turbulence run, produce similar lateral profiles, which are in good agreement with the measured data. Note that the differences in lateral vortex positions for the numerical results are less than the size of scatter in the measured data.

The vertical position history of the vortices, in comparison with the observation, is shown in Figure 4. As expected, results from the two-dimensional simulation show pronounced oscillations in vortex altitude with time, indicating that significant secondary vortices are orbiting around the primary vortices. These oscillations are more significant for the starboard vortex than for the port vortex, since the secondary vortices around starboard vortex have the same sign vorticity to that induced by the ambient crosswind close to the ground. For the numerical simulations with strong turbulence (e.g., the cases with η=0.2349, and η=0.3739), however, the vertical oscillations in vortex positions are much less significant due to dissipation of the secondary vortices by the ambient turbulence. It appears that the vertical movement of the vortices is only weakly sensitive to the level of resolvable-scale turbulence. For example, the maximum difference between simulations for vortex height is only about 10 *m*, as is true for the maximum difference in lateral vortex position. On the other hand, while the observed vortex appears to descend slowly with time, those in the numerical simulations descend initially and then continuously rise almost to the end of simulation time. This discrepancy between observations and numerical results could be caused by the following possibilities: (1) the vortices are embedded in a large-scale downdraft (sinking air surrounding the thermals), note that the case was observed during the early afternoon; (2) the initial profile did not capture the crosswind shear that was local to the actual wake vortex (the gradient in vertical shear can effect the vortex sink rate[4]); (3) the roll-up process is more complex when in ground effect; (4) consequences due to loss-of-lift from the landing aircraft (touchdown occurs near the observing site) or (5) the Lidar observed height is incorrect. The sinking of the wake vortex with a lack of rebound was unexpected, and for this reason, this case was selected for examination. Several other cases observed near this time, showed a vertical trajectory similar to that of the simulations; i.e., rising motion with the vortex approaching a maximum height between ½ b_o to b_o;[24] although according to Delisi,[33] several of the vortices from the DFW IGE cases (one-third to one half) did not appear to rise and remained close to the ground. However, we are unable to determine from our numerical experiments why the observed vortex remained very close to the ground for this event.

Figure 5 shows the time evolution of the axial vorticity field for the baseline case. Note that the magnitude of axial vorticity decreases with time, and by

t = 77 s, the starboard vortex has become almost indistinguishable from the background turbulence. Opposite sign vorticity is generated immediately after initiation by the surface stress at the ground, but the vorticity centers of the secondary vortices are difficult to distinguish from the background turbulence. Figures 6 and 7 show the evolution of the radial profiles for circulation and vorticity for the port vortex. Note that as the vortex decays with time, most of the vorticity remains confined to within a 5 m radius, and that the circulation maintains a more or less uniform radial profile as it decreases with time. However, at larger radii the profile of circulation rapidly diminishes with radius due to contact with the ground. We suspect that turbulence is intensified within this region by Rayleigh instability,[34] and becomes quite efficient in transferring vorticity away from the vortex core.

Sensitivity to Height of Vortex Generation

Three additional experiments are conducted with the height of vortex initiation, Z_i, equal to 2.5 b_o, b_o, and ½ b_o (or equivalently 92.5 m, 37 m, and 18.5 m, respectively). The initial and domain parameters are, otherwise, the same as the previous cases (Tables 1 and 2), except that the crossplane domain width is 9.1 b_o and the crossplane domain height is 3.9 b_o. In order to isolate and easily detect any influences due to the ground, a neutral stratification, a zero mean ambient crosswind, and a somewhat weak ambient turbulence field (η=0.091) are assumed. For comparison and ascertaining the influence of the ground, an additional simulation is conducted which assumes periodic bottom and top boundaries -- and hence, excludes any ground effect.

A comparison of the results (Figs. 7-10) show that the ground can influence the descent rates of vortices at altitudes up to 2.5 b_o; but the 5-10 m averaged circulation is not affected until after the vortex *first* descends (or initiated) below ~0.6 b_o. The results indicate that enhanced decay from ground-effect begins 5-10 seconds after the vortices descend to their minimum height. After which time, the enhanced rate of decay continues, even as the vortices ascend.

For NGE, these results suggest that the descent rate of vortices may be reduced by the influence of the sub-surface vortex images, rather than by a reduction in the average circulation from the ground effect. Vortex decay at these altitudes is primarily influenced by stratification and ambient turbulence.

For IGE, the decay of average circulation is greatly enhanced following the descent of the vortices to their minimum altitude. Beyond this time, the decay process is dominated by the ground interaction, and ambient turbulence has only a secondary influence. However, the ambient turbulence may play a role in reducing the amplitude of the vortex rebound. The amplitude of vortex rebound appears less than in other numerical experiments (cf. Schiling[9], Zheng and Ash[11], and Corjon and Poinsot[13]).

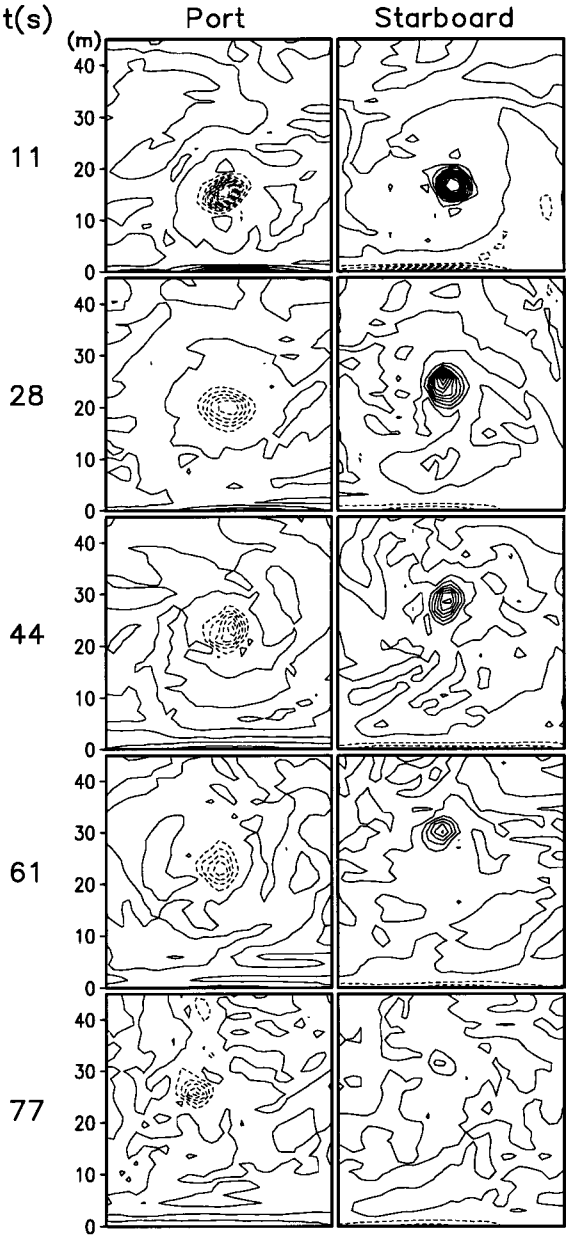

Figure 5. *Time evolution of the axial-component of vorticity within a crossplane for the baseline simulation (η=0.2349). The contour interval for vorticity is 1 s^{-1}.*

Sensitivity to Surface Roughness

In the last set of experiments, sensitivity due to surface roughness is examined. The surface roughness length, z_o, is related to the characteristic roughness of the

ground,[35] and its use in the TASS surface stress formulation is given in the appendix. The sensitivity of this parameter is evaluated by re-running the baseline case with z_o decreased by an order of magnitude.

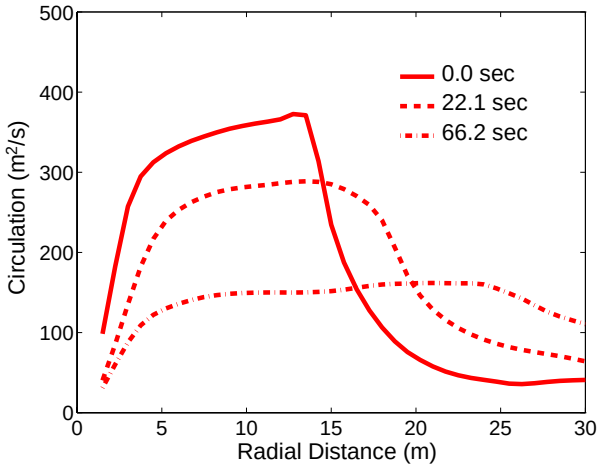

Figure 6. *Radial distribution of circulation for the port vortex of the baseline case at T*=0, 1, and 3 (t = 0, 22, and 66 s). The ground is at radius of 14, 19, and 25m for the three respective times.*

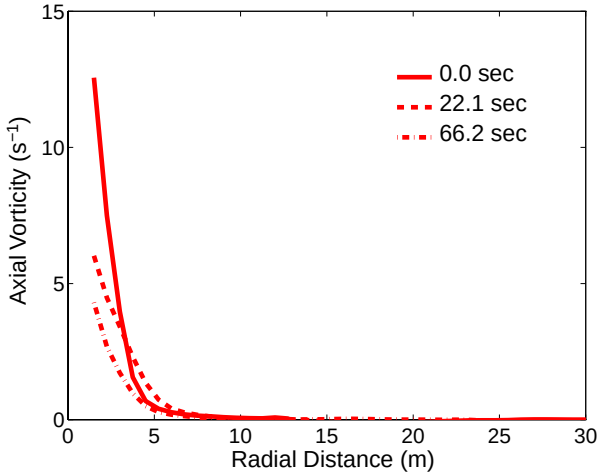

Figure 7. *Same as Fig. 6, but for azimuthal-averaged vorticity.*

The comparisons in Fig. 11 show that the results are weakly affected by an order-magnitude reduction in z_o. However, the results do indicate that a smoother ground weakens the rate of decay and dampens the amplitude of the rebound. A smaller surface roughness could not explain the relatively low vortex trajectory as observed by Lidar for this case.

IV. Summary and Conclusions

A study of wake vortices initialized "in-ground effect," has been performed using a validated LES model. The study is performed with the following limiting assumptions: 1) Crow linking is suppressed due to the truncated axial length of the domain; 2) a simple, post roll-up vortex system is assumed for the initial conditions; 3) the wake vortices are of infinite length; 4) the ambient turbulence is horizontally homogeneous, with the largest scales restricted to the size of the model domain; and 5) the ground is flat with a uniform roughness. The numerical model used in this study differs from that in many previous investigations, in that: 1) time-dependent computations are carried out in three-dimensional space, 2) the computations are LES and at high Reynolds number, 3) realistic surface-stress and subgrid turbulence-closure formulations are assumed, 4) the numerical model has a compressible, non-Boussinesq formulation and a meteorological framework, 5) the model has been validated for real cases, and 6) the numerical formulation is stable, efficient, accurate, and essentially free of numerical diffusion.

Simulations with the three-dimensional LES and with environmental turbulence show strong decay of the vortex average circulation, which agrees very well with the observations, while a two-dimensional simulation without resolvable-scale ambient turbulence largely underestimates the observed rate of decay. For the 3-D cases, the circulation decay appears only weakly sensitive to ambient turbulence levels. The implication for IGE vortex predictions is that crude approximations of ambient turbulence level may be adequate for prediction of circulation decay.

Our LES results also indicate that the lateral and vertical transport of wake vortices is weakly influenced by ambient turbulence, and even a two-dimensional simulation may give good prediction of vortex transport behavior. This conclusion is premised on the absence of large eddy sizes, which can add uncertainty to the vortex trajectory prediction. The IGE numerical results do show good agreement with the measured data, except for the vortex altitude, which remained very, close to the ground in the observed case. Some uncertainties in vortex position data near the ground might be caused by either measurement error or effects from the unresolved features of the large-scale atmospheric flow. The primary conclusions of this study are:

1. Wake vortex transport can be influenced by the ground at altitudes up to 2.5 b_o.
2. Decay of the 5-15 *m* average circulation is directly influenced by the ground following the initial descent below 0.6 b_o. The rate of decay becomes greatly enhanced several seconds after the vortex first reaches its minimum altitude; but prior to this time, the rate of decay is not affected by the ground.
3. Only a weak relation exists between the intensity of ambient turbulence and rate of decay during IGE.

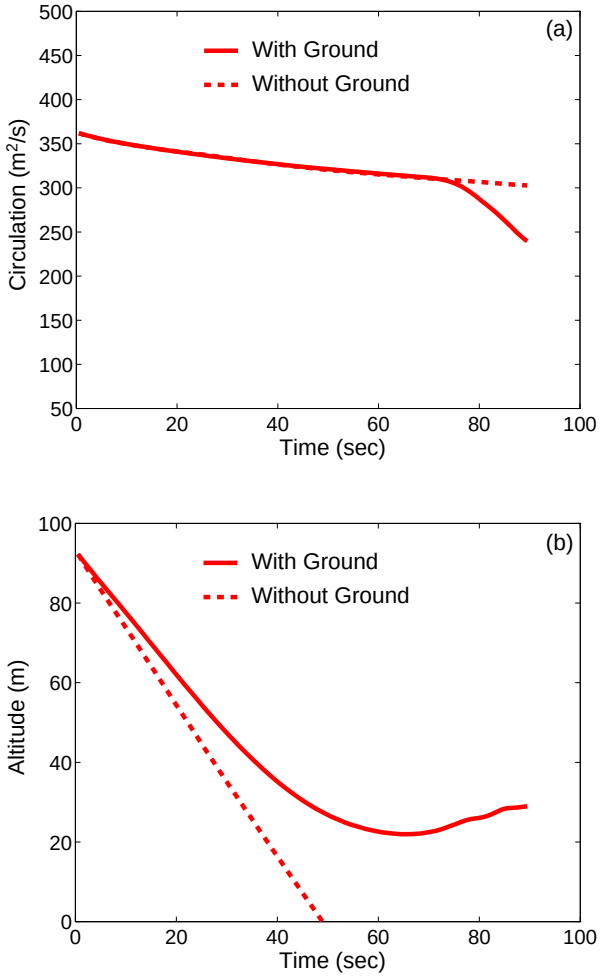

Figure 8. *Time evolution of a) 5-15 m averaged circulation, and b) vortex altitude, for simulation with vortex initiated at Z_i=2.5 b_o. The dashed line represents simulation without ground effect.*

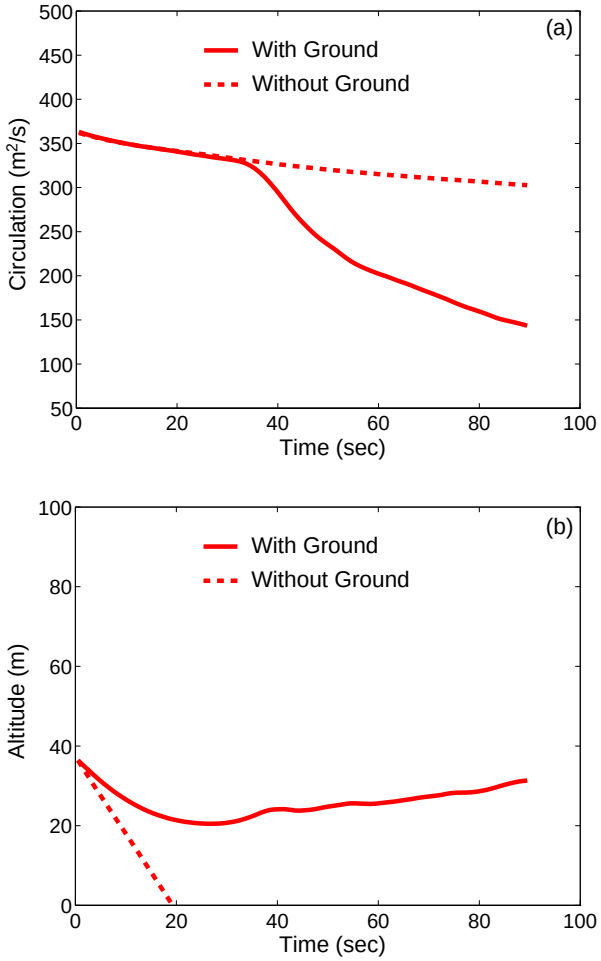

Figure 9. *Same as Fig. 8, but for simulation with wake initiated at Z_i= b_o.*

4. An increase in the surface roughness (and a corresponding increase in surface stress) acts to increase the rate of decay and increase the rebound height of the vortex.
5. Free slip conditions at the ground are inappropriate for models developed for IGE. Viscous stresses reduce the velocity near the surface and act to decouple the primary vortices from their sub-ground images. Ignoring this effect will result in unrealistic divergence of the vortex pairs.

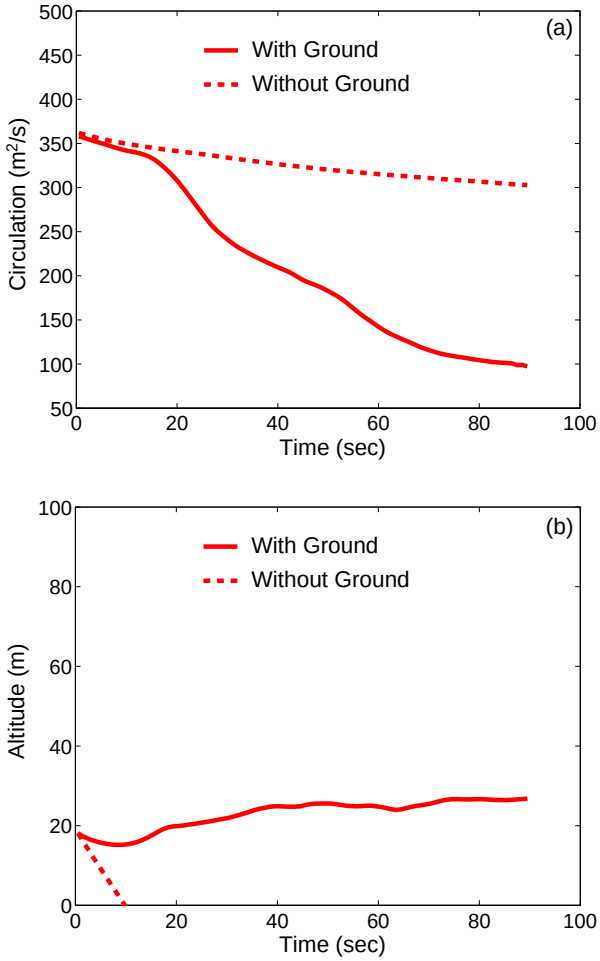

Figure 10. *Same as Fig. 8, but for simulation with wake initiated at Z_i= 0.5 b_o.*

Acknowledgements

This research was sponsored by NASA's Terminal Area Productivity Program. One of the authors was funded under cooperative research grant NCC1-188. Numerical simulations were carried out on NASA and North Carolina Supercomputing Center supercomputers.

Appendix

Formulation for Surface Stress

The following formulation for surface stress was developed during an earlier NASA program and was originally applied to numerical studies of low-level wind shear. This formulation has been used in our wake vortex studies and is applicable to phenomenon having turbulent flow with strong local variations. [Other options for ground boundary conditions are available in TASS,[36] but are not used in our wake vortex simulations.]

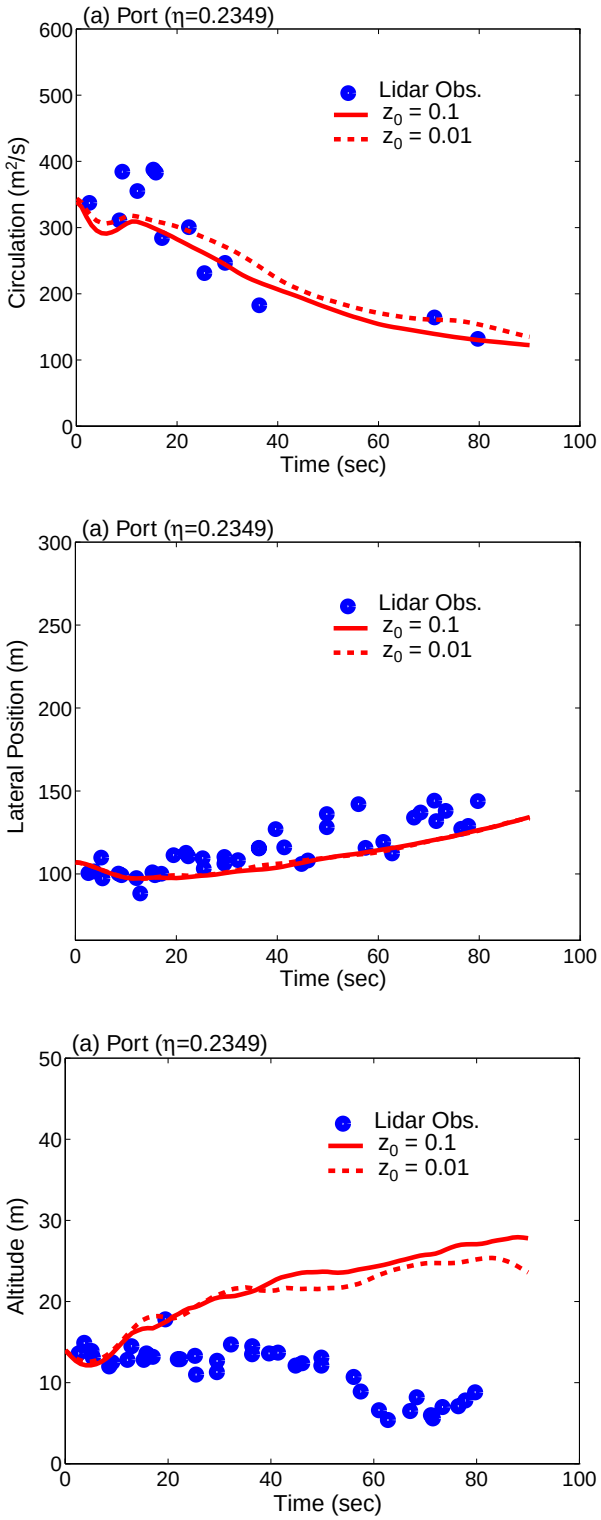

Figure 11. *Sensitivity to surface roughness parameter. Time evolution of a) 5-15 m averaged circulation, b) lateral position and c) vortex altitude for baseline simulation (z_o=0.1m) and simulation with z_o=0.01m.*

The surface stress formulation is used with a nonslip boundary condtion for velocity and a constant flux boundary condition for temperature and vapor. The subgrid stress at the ground (z=0) is computed locally according to:

$$\tau_{uG} = \begin{Bmatrix} Max[\tau_u^*, \overline{\tau_u}(h_1)], & U(h_1) > 0 \\ Min[\tau_u^*, \overline{\tau_u}(h_1)], & U(h_1) \le 0 \end{Bmatrix}$$

where,

$$\tau_u^* \equiv \overline{\tau_u}(h_1) + h_1 \frac{\overline{\tau_u}(h_2) - \overline{\tau_u}(h_1)}{h_2 - h_1},$$

and where, τ_{uG} is the subgrid stress at the ground for the U-component of horizontal velocity, $U(h_1)$ and $U(h_2)$ are the U-components at the first and second grid level above the ground, and h_1 and h_2 are the heights of the respective grid level.

In the above formulation, the local turbulence stresses at levels h_1 and h_2 are averaged horizontally over nine grid points. They are diagnosed as:

$$\tau_u(h) = \frac{\rho U(h) \left|\vec{V}(h)\right| k^2}{\left[\ln(\frac{h - z_o}{z_o}) - \Psi(\frac{h - z_o}{L})\right]^2}$$

where k is von Karmen's constant (=0.4), $|\boldsymbol{V}|$ is the speed of the velocity vector, and Ψ is a nondimensional stability parameter. The Monin-Obukhov (MO) length, L, is determined from the local Richardson number.

The stability parameter can be derived from the MO nondimensional shear functions presented in Hogstrom[37], for stable stratification (L>0):

$\Psi(x) = -5.3\ x$

and for unstable stratification *(L<0):*

$\Psi(x) = 2\ ln\{[1+(1-19x)^{1/4}]/2\} + ln\{[1+(1-19x)^{1/2}]/2\}$
$-2\ \tan^{-1}\{(1-19x)^{1/4}\} + \pi/2$

where $x \equiv (h - z_o) / L$.

The above stability function for unstable stratification is approximated in a more computationally efficient form as:

$\Psi(x) = -0.0627x^5 - 0.6067x^4 - 2.1689x^3 - 3.5874x^2 - 3.1536x$

for $0 < x < -3.5$.

The surface stress for the V-component of horizontal velocity is computed in a similar fashion.

In the above formulation, the turbulence stress at the ground is a function of time and space. Note that either a decrease in the surface roughness, z_o, or an increase in stable stratification reduces the surface stress. Also, for either neutral stratification or strongly sheared flow, that $\Psi \sim 0$, and the surface stress depends only on the wind speed and z_o.

The above formulation was tested in a three-dimensional simulation of a thunderstorm downburst. The numerical simulation was set-up similar to the two-dimensional microburst simulations in Proctor.[38] Strong outflow is generated near the ground as the downdraft impinges upon the surface. An underestimate of the modeled surface stress will result in the outflow maximum being too close to the surface, while an overestimate will displace the maximum too high. Results from the numerical simulation are shown in Figures A1 and A2.

A vertical profile of the local outflow velocity is show in Figure A1. The profile is chosen at the outflow maximum and is compared with a field measurement and a laboratory wall jet. Following Bakke[39], the outflow velocity is normalized by its peak speed and the altitude is normalized by the half-velocity height. Note that the nondimensional profiles are in good agreement, showing the peak velocity at an elevation near 0.25.

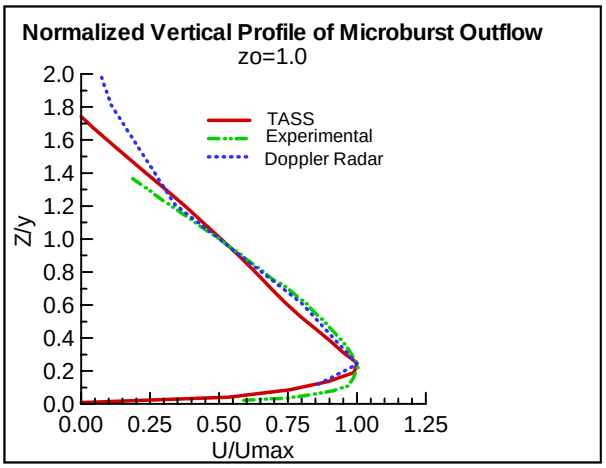

Figure A1. *Nondimensional vertical profile of downdraft outflow. Comparison of 3-D TASS with surface stress formulation with laboratory experiment[39] and a radar field measurement[40].*

In Fig. A2, the profile shows the outflow boundary layer is resolved by 4 grid points and the velocity profile exhibits a log variation with altitude. The intercept for $U = 0$ occurs at $z = 1m$ which agrees with the input

value assumed for z_o. The above comparisons lend support to the suitability of the stress formulation.

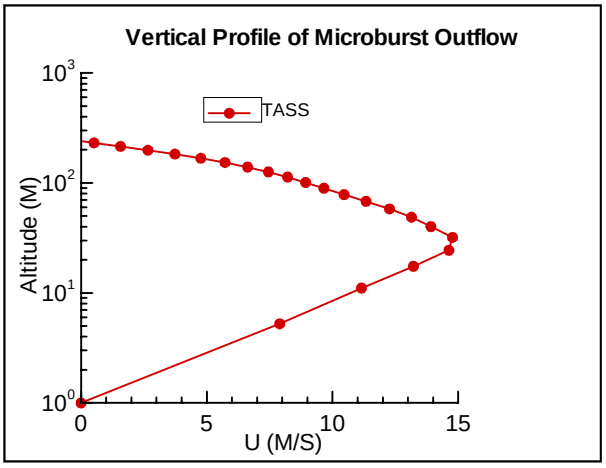

Figure A2. *Log-linear plot of altitude vs outflow speed for TASS simulation. Dots represent the vertical location of the grid points. The profile is chosen within the radius peak outflow.*

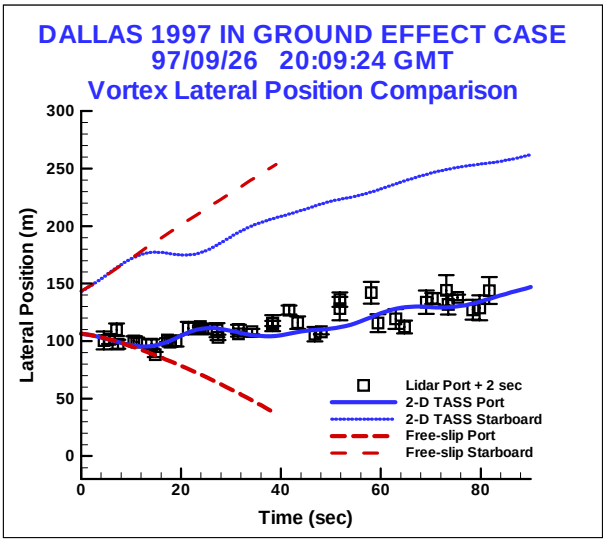

Figure A3. *Comparison of lateral time history for IGE 2-D simulations; results from free-slip (dashed) vs surface stress formulation (solid). Observed locations for the port vortex given by symbols.*

Free-slip vs Surface Stress Boundary Condition

The effects of the surface-stress formulation in comparison with a free-slip condition are evaluated for an IGE case in this section. Two experiments, one for each boundary condition, are conducted with the 2-D version of TASS. The experiments assume no ambient turbulence and a constant grid size of 0.5*m*, with other parameters as defined for the baseline case described in section 2.

A comparison of the time history for the lateral vortex position is shown in Figure A3. For the free-slip condition, the vortices rapidly diverge with the port vortex moving significantly upstream. For the simulation with the surface-stress formulation, the port and starboard vortices separate more slowly. Also, the port vortex moves little and shows good agreement with the location observed with Lidar. Vortex rebound does not occur with the free slip condition but does occur with the surfaces stress formulation. These experiments show that turbulence stress acting at the ground *significantly* affects lateral transport. The proper effects from surface stress should be included within any successful IGE prediction model.

References

[1]Hinton, D.A., "Aircraft Vortex Spacing System (AVOSS) Conceptual Design," NASA Tech. Memo No. 110184, August 1995, 27 pp.

[2]Hinton, D.A., Charnock, J.K., Bagwell, D.R., and Grigsby, D., "NASA Aircraft Vortex Spacing System Development Status," 37th Aerospace Sciences Meeting & Exhibit, Reno, NV,. AIAA-99-0753, January 1999, 17 pp.

[3]Robins, R.E., Delisi, D.P. and Greene, G.C., "Development and Validation of a Wake Vortex Prediction Algorithm," 36th Aerospace Sciences Meeting & Exhibit, AIAA-98-0665, January 1998, 10 pp.

[4]Proctor, F.H., "The NASA-Langley Wake Vortex Modelling Effort in Support of an Operational Aircraft Spacing System," 36th Aerospace Sciences Meeting & Exhibit, AIAA-98-0589, January 1998, 19 pp.

[5]Harvey, J.K., and Perry, F.J., "Flowfield Produced by Trailing Vortices in the Vicinity of the Ground," *AIAA Journal*, Vol. 9, No. 8, August 1971, pp. 1659-1660.

[6]Hallock, J.N., "Wake Vortex Decay Near the Ground," AIAA 8th Fluid and Plasma Dynamics Conf., Hartford, CN, AIAA-75-882, June 1975, 7 pp.

[7]Saffman, P., "The Approach of a Vortex Pair to a Plain Surface in Inviscid Fluid," *Journal of Aircraft*, Vol. 10, No. 11, November 1979, pp. 497-503.

[8]Atias, M. and Weihs, D., "Motion of Aircraft Trailing Vortices Near the Ground," *Journal of Aircraft*, Vol. 21, 1984, pp. 783-786.

[9]Schiling, V.K., "Motion and Decay of Trailing Vortices Within the Atmospheric Surface Layer," *Beitr. Phys. Atmos.*, Vol. 65, May 1992, pp. 157-169.

[10]Robins, R.E. and Delisi, D.P., "Potential Hazard of Aircraft Wake Vortices in Ground Effect with Crosswind," *Journal of Aircraft*, Vol. 30, No. 2, March-April 1993, pp. 201-206.

[11]Zheng, Z.C., and Ash, R.L., "Study of Aircraft Wake Vortex Behavior Near the Ground," *AIAA Journal*, Vol. 34, No. 3, March 1996, pp. 580-589.

[12]Corjon, A., and Stoessel, A., "Three-Dimensional Instability of Wake Vortices Near the Ground," 28th AIAA Fluid Dynamics Conf., Snowmass, CO, AIAA-97-1782, June-July 1997, 14 pp.

[13]Corjon, A. and Poinsot, T., "Behavior of Wake Vortices Near Ground," *AIAA Journal*, Vol. 35, No. 5, May 1997, pp. 849-855.

[14]Wickens, R.H., "A Technique for Simulating the Motion and Ground Effect of Aircraft Wake Vortices," *Canadian Aeronautics and Space Journal*, Vol. 26, No. 2, 1980, pp. 129-133.

[15]Burnham, D.C., and Hallock, J.N., "Measurements of Wake Vortices Interacting with the Ground," 36th Aerospace Sciences Meeting & Exhibit, AIAA-98-0593, January 1998, 12 pp.

[16]Tombach, I., "Observations of Atmospheric Effects on Vortex Wake Behavior," *Journal of Aircraft*, Vol. 10, November 1973, pp. 641-647.

[17]Donaldson, C. duP., and Bilanin, A.J., "Vortex Wakes of Conventional Aircraft," Advisory Group for Aerospace Research & Development, AGARDograph No. 204, May 1975.

[18]Sarpkaya, T., and Daly, J.J., "Effects of Ambient Turbulence on Trailing Vortices," *Journal of Aircraft*, Vol. 24, No. 6, June 1987, pp. 399-404.

[19]Liu, H.-T., "Effects of Ambient Turbulence on the Decay of a Trailing Vortex Wake," *Journal of Aircraft*, Vol. 29, No. 4, April 1992, pp. 255-263.

[20]Sarpkaya, T., "Decay of Wake Vortices of Large Aircraft," *AIAA Journal*, Vol. 36, No. 9, September 1998, pp. 1671-1679.

[21]Han, J., Lin, Y.-L., Arya, S.P., and Proctor, F.H., "Large Eddy Simulation of Aircraft Wake Vortices in a Homogeneous Atmospheric Turbulence: Vortex Decay and Descent," 37th Aerospace Sciences Meeting & Exhibit, AIAA-99-0756, January 1999, 21 pp.

[22]Corjon, A., Zheng, Z.C., and Greene, G.C., "Model of the Behavior of Aircraft Wake Vortices Experiencing Crosswind Near the Ground," 14th AIAA Applied Aerodynamics Conference, New Orleans, LA, AIAA-96-2519, June 1996, 7 pp.

[23]Greene, G.C., "An Approximate Model of Vortex Decay in the Atmosphere," *Journal of Aircraft*, Vol. 23, July 1986, pp. 566-573.

[24]NASA Langley Research Center, "Meteorological & Wake Vortex Data Set, Dallas-Fort Worth International Airport, September 15-October 3, 1997," November 1998, Compact Disc.

[25]Delisi, D.P. and Robins, R.E., Northwest Research Associates, personal communication, September 1998.

[26]Proctor , F.H., "The Terminal Area Simulation System, Volume 1: Theoretical Formulation," NASA Contractor Report 4046, DOT/FAA/PM-85/50, 1, April 1987, 176 pp.

[27]Proctor, F.H., "Numerical Simulation of Wake Vortices During the Idaho Falls and Memphis Field Programs," 14th AIAA Applied Aerodynamics Conference, Proceedings, Part-II, New Orleans, LA, AIAA-96-2496, June 1996, pp. 943-960.

[28]Switzer, G.F., "Validation Tests of TASS for Application to 3-D Vortex Simulations," NASA Contractor Report No. 4756, October 1996, 11 pp.

[29]Han, J., Lin, Y.-L., Schowalter, D.G., Arya, S.P., and Proctor, F.H., "Large Eddy Simulation of Aircraft Wake Vortices in a Homogeneous Atmospheric Turbulence: The Crow Instability," Accepted for publication in *AIAA Journal*.

[30]Crow, S.C., "Stability Theory for a Pair of Trailing Vortices," *AIAA Journal*, Vol. 8, No. 12, December 1970, pp. 2172-2179.

[31]Shen, S., Ding, F., Han, J., Lin, Y.-L., Arya, S.P., and Proctor, F.H., "Numerical Modeling Studies of Wake Vortices: Real Case Simulations," 37th Aerospace Sciences Meeting & Exhibit, AIAA-99-0755, January 1999, 16 pp.

[32]Campbell, S.D., Dasey, T.J., Freehart, R.E., Heinrichs, R.M., Matthews, M.P., Perras, G.H., and Rowe, G.S., "Wake Vortex Measurement Program at Memphis, TN, Data Guide," Project Report: NASA/L-2, January, 1997 (also in NASA CR-201690, April 1997).

[33]Delisi, D., Northwest Research Associates, personal communication, December 1998.

[34]Rayleigh, L., "On the Dynamics of Revolving Fluids," *Proc. Royal Soc. London*, A, Vol. 93, 1917, pp. 148-154 (also in *Scientific Papers*, Vol. 6, pp. 447-453).

[35]Stull, R.B., *An Introduction to Boundary Layer Meteorology*, Kluwer Academic Publishers, 1988.

[36]Schowalter, D.G., DeCroix, D.S., Lin, Y.-L., Arya, S.P., and Kaplan, M.L., "The Sensitivity of Large-Eddy Simulation to Local and Nonlocal Drag Coefficients at the Lower Boundary," NASA Contractor Report 198310, April 1996, 43 pp.

[37]Hogstrom, U., "Review of Some Basic Characteristics of the Atmospheric Surface Layer," *Boundary-Layer Meteorology*, Vol. 78, 1996, pp. 215-246.

[38]Proctor, F.H., "Numerical Simulation of an Isolated Microburst. Part I: Dynamics and Structure," *J. Atmos. Sci.*, Vol 45, No. 21, November 1988, pp. 3137-3160.

[39]Bakke, P., "An Experimental Investigation of a Wall Jet," *J. Fluid Mech.*, Vol. 2, 1957, pp. 467-472.

[40] Fujita, T.T., 1981, "Tornadoes and Downbursts in the Context of Generalized Planetary Scales," *J. Atmos. Sci.*, Vol. 38, 1981, pp. 1511-1534.